Redox Biology 62 (2023) 102652

Contents lists available at ScienceDirect

Redox Biology

journal homepage: www.elsevier.com/locate/redox

SIRT3 improved peroxisomes-mitochondria interplay and prevented cardiac hypertrophy via preserving PEX5 expression

Minghui Wang [a,1], Yanqing Ding [a,b,1], Yuehuai Hu [a], Zeyu Li [a], Wenwei Luo [a,c], Peiqing Liu [a,**], Zhuoming Li [a,*]

[a] Department of Pharmacology and Toxicology, School of Pharmaceutical Sciences, National and Local United Engineering Lab of Druggability and New Drugs Evaluation, Guangdong Engineering Laboratory of Druggability and New Drug Evaluation, Guangdong Provincial Key Laboratory of New Drug Design and Evaluation, Sun Yat-sen University, China

[b] School of Medicine, Kunming University of Science and Technology, China

[c] Department of Pharmacy, Guangdong Provincial People's Hospital (Guangdong Academy of Medical Sciences), Southern Medical University, China

ARTICLE INFO

Keywords:
SIRT3
PEX5
Cardiomyocyte hypertrophy
Mitochondria-peroxisomes crosstalk

ABSTRACT

The present study identified a novel mechanism underlying the protective effect of Sirtuin 3 (SIRT3) against pathological cardiac hypertrophy, beyond its well-accepted role as a deacetylase in mitochondria. SIRT3 modulates the peroxisomes-mitochondria interplay by preserving the expression of peroxisomal biogenesis factor 5 (PEX5), thereby improving mitochondrial function. Downregulation of PEX5 was observed in the hearts of *Sirt3*$^{-/-}$ mice and angiotensin II-induced cardiac hypertrophic mice, as well as in cardiomyocytes with SIRT3 silencing. PEX5 knockdown abolished the protective effect of SIRT3 against cardiomyocyte hypertrophy, whereas PEX5 overexpression alleviated the hypertrophic response induced by SIRT3 inhibition. PEX5 was involved in the regulation of SIRT3 in mitochondrial homeostasis, including mitochondrial membrane potential, mitochondrial dynamic balance, mitochondrial morphology and ultrastructure, as well as ATP production. In addition, SIRT3 alleviated peroxisomal abnormalities in hypertrophic cardiomyocytes via PEX5, as implied by improvement of peroxisomal biogenesis and ultrastructure, as well as increase of peroxisomal catalase and repression of oxidative stress. Finally, the role of PEX5 as a key regulator of the peroxisomes-mitochondria interplay was confirmed, since peroxisomal defects caused by PEX5 deficiency led to mitochondrial impairment. Taken together, these observations indicate that SIRT3 could maintain mitochondrial homeostasis by preserving the peroxisomes-mitochondria interplay via PEX5. Our findings provide a new understanding of the role of SIRT3 in mitochondrial regulation via interorganelle communication in cardiomyocytes.

1. Introduction

SIRT3, a member of the silent information regulator 2α (SIR2α)-related protein Sirtuins (SIRTs) family, has emerged as a novel and promising therapeutic target for pathological cardiac hypertrophy [1,2]. Deficiency of SIRT3 facilitates the development of cardiac hypertrophy and heart failure [3]. Mechanisms underlying the cardioprotective effects of SIRT3 mainly focus on its role as a deacetylase that deacetylates mitochondrial proteins participating in the TCA cycle [4,5], redox balance [6], electron transport [7], fatty acid metabolism [8] and mitochondrial dynamics [9]. However, recent studies indicate that SIRT3 could also serve as a coordinator of mitochondria-nuclear retrograde signals, which refers to a wide range of retrograde signals generated from the mitochondria to alter the expression of nuclear genes involved in metabolic reprogramming or stress defense [10,11]. SIRT3 might coordinate retrograde signals in three different ways. First, SIRT3

Abbreviations: ANF, atrial natriuretic factor; Ang II, angiotensin II; β-MHC, myosin heavy chain β; CAT, catalase; DHE, dihydroethidium; Drp1, dynamin-related protein 1; Mfn2, mitofusin 2; MMP, mitochondrial membrane potential; NRCM, neonatal rat cardiomyocytes; PE, phenylephrine; PEX5, peroxisomal biogenesis factor 5; PMP70, peroxisomal membrane protein 70 kDa; TEM, transmission electron microscope; 3-TYP, 3-(1H-1,2,3-triazol-4-yl) pyridine.

* Corresponding author. Department of Pharmacology and Toxicology, School of Pharmaceutical Sciences, Sun Yat-sen University, 132# East Wai-huan Road, Higher Education Mega Center, Guangzhou, 510006, Guangdong, China.

** Corresponding author.

E-mail addresses: liupq@mail.sysu.edu.cn (P. Liu), lizhm5@mail.sysu.edu.cn (Z. Li).

[1] These authors contributed equally: Minghui Wang and Yanqing Ding.

https://doi.org/10.1016/j.redox.2023.102652
Received 4 February 2023; Received in revised form 23 February 2023; Accepted 27 February 2023
Available online 4 March 2023

enhances the mitochondrial unfolded protein response (UPR^{mt}), which is a form of retrograde mito-nuclear communication that is responsible for quality control of the mitochondrial proteome [12–14]. Second, SIRT3 deacetylates transcription factors such as FOXO3a [15], FOXO1 [16] and GSK3β [17] in mitochondria to facilitate their nuclear or cytoplasmic translocation, ultimately regulating target gene expression. Third, SIRT3 can be distributed in the nucleus, although it is mainly located in mitochondria [18–20]. The distribution of SIRT3 in the nucleus is promoted in response to the stress response, for instance, isoproterenol stimulation in cardiomyocytes [21]. SIRT3 in the nucleus is able to regulate gene expression by deacetylating histones, including H3K27Ac [22], H3K9Ac and H4K16Ac [19,20], or nuclear proteins, such as PARP-1 [21] and Ku70 [23]. These findings thus prompt the hypothesis that SIRT3 might regulate cellular function by affecting nuclear gene expression during cardiac hypertrophy, in addition to its well-known deacetylation function in mitochondria.

Therefore, the present study conducted an mRNA microarray analysis in hearts from cardiac hypertrophic mice and *Sirt3* knockout mice to screen out genes potentially regulated by SIRT3. According to the results, peroxisomal biogenesis factor 5 (PEX5) was found to be remarkably downregulated when SIRT3 was deficient. PEX5, the fifth member of the protein family involved in the biogenesis of peroxisomes, is mainly responsible for transporting matrix proteins from the cytoplasm into the peroxisomal matrix [24]. PEX5 forms a protein complex with proteins containing peroxisomal targeting signal 1 (PTS1) sequences at the C-terminus to carry these proteins into peroxisomes [24]. Since these PEX5 cargoes are widely involved in peroxisomal fatty acid oxidation, peroxisomal assembly, catabolism of reactive oxygen, and synthesis of ether phospholipid species [25], PEX5 is pivotal in the regulation of peroxisomal function. Indeed, defects in PEX5 could lead to peroxisomal biogenesis diseases such as Zellweger syndrome [26]. Currently, the role of PEX5 in cardiovascular diseases is rarely reported. Observations from $PEX5^{-/-}$ mice show that cardiac metabolism was altered due to peroxisomal deficiency and mitochondrial dysfunction [27]. Additionally, patients with Refsum's disease, which is a typical peroxisomal biogenesis disease, exhibited tachycardia, gallop rhythm, systolic murmurs, enlargement of the heart, cardiac insufficiency and heart failure [28,29]. These evidences imply that defects in PEX5 might facilitate the pathogenesis of cardiac diseases.

The present study was designed to investigate whether PEX5 was involved in the inhibitory effect of SIRT3 on cardiac hypertrophy. Interestingly, peroxisomes and mitochondria exhibit a close functional interplay to coordinate multiple bioactivities, including fatty acid metabolism, redox homeostasis, membrane dynamics and antiviral signaling [30]. Since SIRT3 is crucial for mitochondrial function and PEX5 is a key regulator of peroxisomal function, the present study also explored the hypothesis that SIRT3 could improve peroxisomes-mitochondria interplay by preserving PEX5 expression.

2. Materials and methods

2.1. Animal experiments

Male *Sirt3* knockout mice (Strain# 129-$Sirt3^{tm1.1Fwa}$/J) and their age-, sex- and background-matched wild-type (WT) control (129/SvlmJ) mice were purchased from Jackson Laboratory (Bar Harbor, ME, USA). To generate an *in vivo* model of cardiac hypertrophy, adult male WT mice (10–12 weeks old) were subjected to chronic subcutaneous infusion of Ang II (2 mg kg^{-1} d^{-1} dissolved in 0.9% NaCl, No. A9525, Sigma–Aldrich, Saint Louis, MO, USA). The control group was infused with an equal volume of normal saline (NS). All animals were subcutaneously infused with Ang II or NS by implanted osmotic minipumps (Alzet model 1002, Alza Corp.) for 2 weeks. $Sirt3^{-/-}$ mice (male, 28 weeks old) and their matched WT mice were used to evaluate the pro-hypertrophic effect of SIRT3 deficiency. Animals were sacrificed and subjected to hypertrophic response analysis. Experimental animals were housed in individually ventilated cages in a specific pathogen-free (SPF) facility with a 12:12 h light/dark cycle and room temperature of 21–23 °C. All animal experiments complied with the ARRIVE guidelines. Animal protocols and care procedures were approved by the Research Ethics Committee, Sun Yat-sen University and were conducted in accordance with the Guide for the Care and Use of Laboratory Animals (NIH Publication No. 85-23, revised 1996). Microarray analysis of differentially expressed mRNA levels was conducted by KangChen Biotech (Shanghai, China).

2.2. Echocardiography analysis and morphometric measures

Animals were anesthetized with 3% (v/v) isoflurane, and two-dimensional-guided M-mode echocardiography was performed using a Technos MPX ultrasound system (ESAOTE, SpAESAOTE SpA, Italy) (Vevo 2100 equipped) by an operator who was blinded to the design of the experiment. Afterwards, the mice were sacrificed, and the hearts were rapidly isolated for further analysis. For morphological measurements, mouse hearts were arrested by injection of 0.1 mM KCl solution at end-diastole and carefully excised for weighing and photographing; heart weight was displayed as a ratio to body weight. Hearts were transected, and the transverse sections were fixed in 4% paraformaldehyde, embedded in paraffin and stained with hematoxylin-eosin (HE) for histological analysis.

2.3. Primary culture of neonatal rat cardiomyocytes

Neonatal rat cardiomyocytes (NRCMs) were prepared from 1-3-day-old Sprague–Dawley (SD) rats obtained from the Experimental Animal Facility of Sun Yat-sen University. Anesthetized SD rats were sacrificed before their hearts were excised and washed three times in precooled sterile PBS. Ventricles were cut into approximately 1 mm^3 pieces and immersed in 12.5 ml 0.08% trypsin solution at 37 °C for 4–6 min each time, with magnetic stirrer stirring at 250–300 r/min. After 12–16 rounds of digestion, cell suspensions were collected following centrifugation for 5 min at 1600×*g* before cell pellets were suspended in Dulbecco's modified Eagle's medium (DMEM) (Gibco BRL, Grand Island, NY, USA) containing 10% fetal bovine serum (FBS) (Gibco BRL, Grand Island, NY, USA). To remove fibroblasts, cells were preplated into flasks for 1 h. Then, unattached NRCMs were seeded at a density of 1×10^6 cells/well into 6-well plates, cultivated in DMEM with 10% FBS and 0.1 mM 5-bromodeoxyuridine, and incubated in a humidified atmosphere of 95% air/5% CO_2 at 37 °C.

2.4. Immunoblot analyses

Heart tissues or NRCMs were lysed in Western and IP lysis buffer (Beyotime, Haimen, China) supplemented with 1 mM protease and phosphatase inhibitors (Invitrogen, Carlsbad, CA, USA) to extract protein at 4 °C for 30 min. The lysates were centrifuged at 12,000 g at 4 °C for 15 min after sonicating or vortexing, and the supernatants were collected. Protein concentrations were measured by a BCA Protein Assay Kit (Thermo Fisher Scientific, Waltham, MA, USA). Equal amounts of protein samples were separated by sodium dodecyl sulfate–polyacrylamide gel electrophoresis (SDS–PAGE) and transferred to a polyvinylidene difluoride (PVDF) membrane (Millipore, CA, USA). The membrane was blocked with 5% non-fat milk prepared in Tris buffered saline Tween (TBST) (Boster, Wuhan, China) for 60 min at room temperature before being incubated with primary antibodies overnight at 4 °C and the secondary antibodies at room temperature for 1 h. The blots were visualized by enhanced chemiluminescence reagents (Tanon, Shanghai, China), and the immunoreactive bands were detected by a chemical imaging system (Tanon, Shanghai, China). The intensity of the bands was measured by ImageJ software (National Institutes of Health, Bethesda, MD, USA).

2.5. Measurement of superoxide

Live NRCMs were incubated with 10 μM 2,7-diamino-10-ethyl-9-phenyl-9,10-dihydrophenanthridine (DHE) dye (Beyotime, Hangzhou, China) according to the manufacturer's instructions. Fluorescence images were acquired by fluorescence microscopy (EVOS FL Auto, Life Technologies, Bothell, WA, USA), and the fluorescence intensity was calculated by a High-Content Screening System (ArrayScanVTI, Thermo Fisher Scientific, Rockford, IL, USA).

2.6. Detection of mitochondrial membrane potential (MMP) using JC-1 staining

NRCMs were incubated for staining with 10 μM JC-1 probe (Beyotime, Hangzhou, China) according to the manufacturer's instructions. Images were captured using a fluorescence microscope (EVOS FL Auto, Life Technologies, Bothell, WA, USA), and fluorescence intensity was calculated by a High-Content Screening System (ArrayScanVTI, Thermo Fisher Scientific, Rockford, IL, USA).

2.7. Total RNA extraction and quantitative real-time polymerase chain reaction (qRT–PCR)

Total RNA was extracted using TRIzol reagent according to the manufacturer's instructions. Five micrograms of total RNA was reverse transcribed into cDNA according to the protocol of the reverse transcription kit (Thermo Fisher Scientific, Waltham, MA, USA). The mRNA levels of the target genes were reflected by the cycle time (Ct) values determined by a SYBR Green Quantitative PCR kit (Thermo Fisher Scientific, Waltham, MA, USA) in a real-time PCR amplifier (Thermo Fisher Scientific, Waltham, MA, USA). The real-time quantitative PCR procedures were as follows: predenaturation at 94 °C for 3 min, followed by 40 cycles of 94 °C for 45 s, 58 °C for 30 s, and 72 °C for 30 s, with a final extension at 72 °C for 5 min. Primers for target genes were synthesized by Sangon Biotech Co Ltd. (Shanghai, China), and the sequences are listed in Table 1 β-Actin served as an endogenous control. Data are expressed as the fold change over the control group.

2.8. Measurement of cell surface area

NRCMs were seeded in 6-well plates. The culture medium was discarded, and the cells were fixed with 4% paraformaldehyde for 20 min at room temperature. After that, fixed cells were incubated with 0.1% rhodamine-phalloidin (Invitrogen, Carlsbad, CA, USA) for 30 min. Cells were washed with PBS and further incubated with 4',6-diamidino-2-phenylindole (DAPI) (Invitrogen, Carlsbad, CA, USA) for 10 min. The cell surface area was calculated by a High-Content Screening System (Thermo Fisher Scientific, Rockford, IL, United States). Fluorescence images were acquired by an Array Scan VII HCS Reader (Thermo Fisher Scientific, Rockford, IL, United States).

2.9. RNA interference

Small interfering RNAs (siRNA) were synthesized by Genepharma (Shanghai, China). NRCMs seeded in 6-well plates were transfected with 100 pmol of siRNA (negative control siRNA for the control group) in 3 μL of Lipofectamine RNAiMAX reagent (Invitrogen, Carlsbad, CA, USA) according to the manufacturer's instructions. After that, cells were harvested to perform Western blotting to compare the silencing efficiency of different siRNAs. The sequences of *Pex5* siRNA and negative control siRNA are listed in Table 2.

2.10. Plasmid transfection

PEX5-Flag (PEX5) was obtained from GeneChem (Shanghai, China). NRCMs seeded in 6-well plates were transfected with 2 μg of plasmid (vector for negative control) assisted by 5 μL lipofectamine 2000 (Invitrogen, Carlsbad, CA, USA). Cells were harvested to perform Western blotting to test overexpression efficiency.

2.11. Transmission electron microscope (TEM) image capture

To morphologically confirm the structure of mitochondria and peroxisomes, ultrastructure analysis was conducted as previously described [31]. In brief, NRCMs were scraped with a cell scraper and collected in EP tubes by centrifugation at 1000×*g* for 5 min. Then, 2.5% glutaraldehyde (PanEra, Guangzhou, China) was added to fix the cells at 4 °C for 2 h, and the cells were postfixed with 1% osmium tetroxide (Electron Microscopy Sciences, Hatfield, PA, USA). After dehydration by a graded concentration series of ethanol, NRCMs were embedded in Embed812 resin. The resin was sectioned into 75 nm thick sections. The ultrathin sections were mounted on copper grids and then double-stained with uranyl acetate (E. Merck, Darmstadt, Germany) and lead citrate (Sigma–Aldrich, St. Louis, MO, USA). The images of cellular organelles were observed and captured by a JEM-1400 Electron Microscope (JEOL Ltd., Japan).

2.12. ATP content analysis

ATP content in NRCMs was detected using an assay kit (Beyotime, Shanghai, China) with luciferase according to the manufacturer's instructions. In short, NRCMs were seeded in 24-well plates. After treatment, the cells were lysed with ATP lysis buffer, and the supernatant was collected by centrifugation at 12000 rpm for 5 min. Supernatant samples were mixed with luciferase solution, and chemiluminescence was detected. The ATP concentration was normalized to the protein content. Data are shown as the level relative to the control.

Table 2
The sequence of siRNA used for RNA interference.

Target gene	Sense (5′-3′)	Antisense (5′-3′)
Negative control siRNA	UUCUCCGAACGUGUCACGUTT	ACGUGACACGUUCGGAGAATT
PEX5 siRNA	GCGCCAUGUCUGAGAACAUTT	AUGUUCUCAGACAUGGCGCTT
SIRT3 siRNA	CAGCAAGGUUCUUACUACATT	UGUAGUAAGAACCUUGCUGTT

Table 1
List of primers for qPCR analysis.

Genes	Primer (Forward)	Primer (Reverse)
β-actin	TCGTGCGTGACATTAAAGAG	ATTGCCGATAGTGATGACCT
Rasgrf2	CACAGCAGCAGCAGGACATGG	TGGCGGAGGACATTCAGGACTC
Irf9	CTCGCTGCTGCTCACCTTCATC	AGCCACAAGCCGACAGTCTAGG
Pex5	CTTGCCGCTGGAGATGCTGTG	TCGGTCAGTGGTAGAGGTTCCTTC
Ramp1	TCTCATCCAGGAGCTGTGTCTCAG	GTAGCGGTGGTGGACAGCAATG
Prkg1	GCTGCCTTCTTCGCCAACCTG	TGCTCCTGCTGTCTCGTGTCC
Plimd5	AGGCGATGTGGTTCTCAGCATTG	CTCAGACTTGGCAGCAGCAGAAG
Hnrnpd	GAGCTGCCTATGGACAACAAGACC	CCACTGCTGCTGCTGCTGATAC

2.13. Immunofluorescence (IF) assay

NRCMs seeded on 48-well plates were washed with warm PBS and fixed with 4% paraformaldehyde for 20 min at room temperature. After washing with PBS three times, the cells were permeabilized with 0.3% Triton X-100 (Sangon Biotech, Shanghai, China, # A110694) for 15 min at room temperature. Cells were washed three times and subsequently incubated in 10% goat serum (BOSTER, Wuhan, China, # AR0009) as blocking solution for 1 h at room temperature. Then, NRCMs were further treated with blocking solution containing primary antibody overnight at 4 °C. After that, NRCMs were incubated with Alexa Fluor-labeled secondary antibody for 1 h at room temperature. DAPI (1 μg/mL, Sigma–Aldrich, St. Louis, MO, #D9542) was used to stain nuclei at room temperature for 5 min. Fluorescence images were acquired by

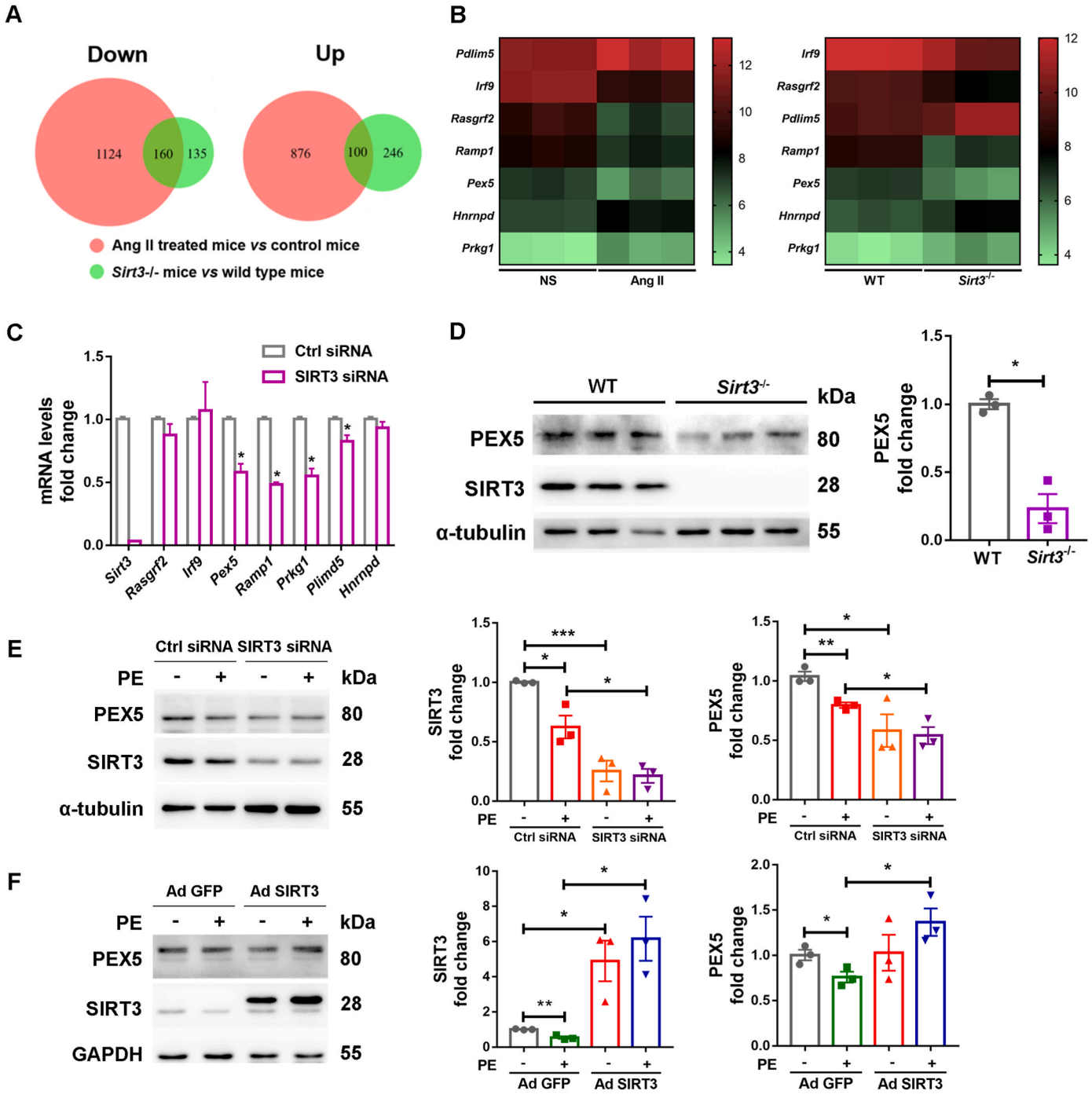

Fig. 1. SIRT3 regulated PEX5 expression level in cardiomyocyte hypertrophy. (A) Venn diagrams showed the number of differentiated expression genes from heart tissue extracted from Ang II induced cardio-hypertrophic mice (WT mice, male, 10–12 weeks old) and *Sirt3* knock out mice (male, 28 weeks old). **(B)** The heat maps showed the alteration of expression level of selected genes according to microarray analysis results. Values of normalized intensity for differentiated genes was there for comparison. **(C)** qPCR validation result of selected genes at cellular level by silencing SIRT3 in NRCMs. **(D)** The protein level of PEX5 in heart tissue from SIRT3 KO mice and wild type mice were measured by Western blot. **(E)** NRCMs were transfected with SIRT3 siRNA with or without PE treatment (Ctrl siRNA was used as negative control). The protein level of SIRT3 and PEX5 was examined by Western blot. **(F)** NRCMs were infected by Ad SIRT3 with or without PE treatment (Ad GFP was used as negative control). The protein level of SIRT3 and PEX5 was tested by Western blot. All data were showed as the means ± SEM. $^{*}P < 0.05$. $^{**}P < 0.01$. $^{***}P < 0.001$. $n = 3$.

using a fluorescence microscope (EVOS FL Auto, Life Technologies, Bothell, WA, USA), and the fluorescence intensity was calculated by a High-Content Screening System (ArrayScanVTI, Thermo Fisher Scientific, Rockford, IL, USA).

2.14. Mitochondrial network analysis

NRCMs were seeded in glass cell culture dishes, and the mitochondrial network was stained with 200 nM Mitotracker-red dye (Invitrogen, Carlsbad, CA, USA) according to the manufacturer's instructions. NRCMs were incubated at 37 °C for 20 min. Images were captured by laser scanning microscopy (Olympus Corporation, Japan), and mitochondria were analyzed by ImageJ as previously described [32].

2.15. Statistical analysis

Data are presented as the means ± SEMs. Differences between two groups were analyzed by two-tailed unpaired Student's *t*-test between two groups, and one-way ANOVA followed by the Bonferroni post hoc test was used for multiple comparisons. Statistical analyses were conducted by GraphPad Prism 7.0 (GraphPad Software, La Jolla, CA, USA). $P < 0.05$ was considered statistically significant.

3. Results

3.1. The expression of PEX5 was downregulated in SIRT3-deficient cardiac hypertrophic models in vitro and in vivo

Twenty-eight-week-old *Sirt3* knockout mice displayed significant cardiac hypertrophy and heart failure phenotypes, as implied by the increased size of hearts, disarrangement of cardiomyocytes and deposition of collagen, decrease in ejection fraction (EF%) and fraction shortening (FS%), as well as increase in heart weight (HW)/body weight (BW) ratio (Fig. S1) [33–35]. Similarly, Ang II treatment for 2 weeks in wild-type mice also led to a remarkable cardiac hypertrophic response and downregulation of SIRT3 (Fig. S2) [34,35]. To screen out genes that were potentially regulated by SIRT3 in cardiac hypertrophy, mRNA microarray analysis was conducted in hearts from 28-week-old *Sirt3* global knockout mice and Ang II-induced cardiac hypertrophic mice. As shown in Fig. 1A, 160 downregulated genes and 100 upregulated genes overlapped in both Ang II-treated mice and SIRT3 knockout mice (**Supplementary data 2**). Among them, 7 genes (*Rasgrf2*, *Irf9*, *Pex5*, *Ramp1*, *Prkg1*, *Plimd5*, *Hnrnpd*) demonstrated significant alterations in hypertrophic mice or SIRT3 knockout mice compared to control/wild-type mice (Fig. 1B) and thus were selected for qPCR validation in SIRT3-silenced NRCMs. Our data showed that the mRNA level of PEX5 was significantly decreased by SIRT3 knockdown, consistent with the microarray results (Fig. 1C). Additionally, the protein expression of PEX5 was decreased in the hearts of SIRT3 knockout mice (Fig. 1D). Moreover, the expression of PEX5 was repressed in PE-induced hypertrophic cardiomyocytes, which demonstrated a downregulation of SIRT3 (Fig. 1E and F). SIRT3 silencing exacerbated the PE-induced downregulation of PEX5 (Fig. 1E), whereas SIRT3 overexpression reversed the reduction in PEX5 (Fig. 1F). Therefore, these *in vitro* and *in vivo* results support the conclusion that PEX5 expression is under the regulation of SIRT3 and that PEX5 is downregulated when SIRT3 is deficient.

3.2. PEX5 was involved in the protective effect of SIRT3 against cardiomyocyte hypertrophy

Since SIRT3 is well-known for its protective effect against cardiac hypertrophy [1,2] and our previous study showed that PEX5 could inhibit cardiomyocyte hypertrophy [36], the potential involvement of PEX5 in the cardioprotective effect of SIRT3 was elucidated. In PE-treated cardiomyocytes, overexpression of SIRT3 suppressed the increased expression of the hypertrophic markers atrial natriuretic factor (ANF) and β myosin heavy chain (β-MHC), as well as the increase in cell surface area (Fig. 2A & C). However, knockdown of PEX5 abolished the anti-hypertrophic effect of SIRT3 (Fig. 2A & C). In contrast, overexpression of PEX5 reversed the upregulation of ANF and β-MHC and the enlargement of cardiomyocytes induced by the SIRT3 inhibitor 3-TYP (Fig. 2B & D), suggesting that PEX5 attenuates the detrimental effect of SIRT3 inhibition on cardiomyocyte hypertrophy. Thus, these observations indicate that PEX5 is at least partially involved in the beneficial effect of SIRT3 in cardiomyocytes.

3.3. PEX5 was required for SIRT3's protective effect on mitochondria

SIRT3 is well-known as a key regulator of mitochondrial function [37]. To elucidate how PEX5 participates in the anti-hypertrophic effect of SIRT3, the involvement of PEX5 in the regulatory effect of SIRT3 on mitochondrial function was investigated. First, the mitochondrial membrane potential (MMP) was measured by JC-1 staining in NRCMs combined with SIRT3 overexpression and PEX5 knockdown, or with SIRT3 inhibition and PEX5 overexpression. As displayed in Fig. 3A, SIRT3 overexpression restored PE-induced disruption of MMP, while this effect was blocked by PEX5 knockdown. Conversely, the diminished MMP was exacerbated by the SIRT3 inhibitor 3-TYP, but was remarkably improved when PEX5 was overexpressed (Fig. 3B). Second, mitochondrial dynamics were determined by measuring the expression of the mitochondrial fission protein Drp1 and fusion protein Mfn2. In PE-stimulated cardiomyocyte hypertrophy, Drp1 was upregulated, while Mfn2 was downregulated, indicating that the dynamic balance of mitochondrial fusion and fission was destroyed, switching from fusion to fission (Fig. 3C). SIRT3 overexpression prevented the defective mitochondrial dynamics in cardiomyocyte hypertrophy, but this beneficial effect was abrogated if PEX5 was deficient (Fig. 3D). In contrast, supplementation with PEX5 suppressed mitochondrial fission but promoted mitochondrial fusion in the presence of the SIRT3 inhibitor (Fig. 3E). Third, the morphology of the mitochondrial network was visualized by the mitochondrion-specific dye Mitotracker-red. As shown in Fig. 3F and G, normal cardiomyocytes possess a dense mitochondrial network that extends through the cytoplasm, whereas PE stimulation led to mitochondrial fragmentation with punctate morphology. Mitochondrial morphological analysis showed an increased ratio of fragmented mitochondria and elevated mitochondrial number but diminished mitochondrial volume in cardiomyocytes treated with PE (Fig. 3F and G). SIRT3 overexpression resulted in less fragmented mitochondria, less space network, fewer discrete dots and more elongated lines or branches, suggesting that SIRT3 could inhibit mitochondrial fragmentation triggered by PE (Fig. 3F). However, this beneficial effect was reversed in the absence of PEX5 (Fig. 3F). Conversely, mitochondrial network disruption was deteriorated by 3-TYP, but recovered by PEX5 overexpression (Fig. 3G). Fourth, the change in mitochondrial ultrastructure was observed by TEM. As shown in Fig. 3H and I, normal mitochondrial ultrastructure was characterized by a bilayer membrane and tightly stacked cristae. In hypertrophic cardiomyocytes, the mitochondria became intumesced, and their inner membrane became swollen, vague and fragmented (Fig. 3H and I). The impaired mitochondrial ultrastructure induced by PE was attenuated by SIRT3 overexpression but was worse if PEX5 was deficient (Fig. 3H). Mitochondrial ultrastructural destruction was aggravated by SIRT3 inhibition but was restored by PEX5 overexpression (Fig. 3I). Finally, ATP content was measured to assess the function of mitochondria. Under stimulation by PE, ATP levels in cardiomyocytes were increased, which might be attributed to promoted mitochondrial fission and increased mitochondrial number (Fig. 3J and K). SIRT3 significantly resisted the elevation of ATP content (Fig. 3J), whereas PEX5 deficiency inhibited the effect of SIRT3 and rebound ATP production (Fig. 3J). In contrast, SIRT3 inhibition exacerbated the excess production of ATP, which could be overridden by PEX5 (Fig. 3K).

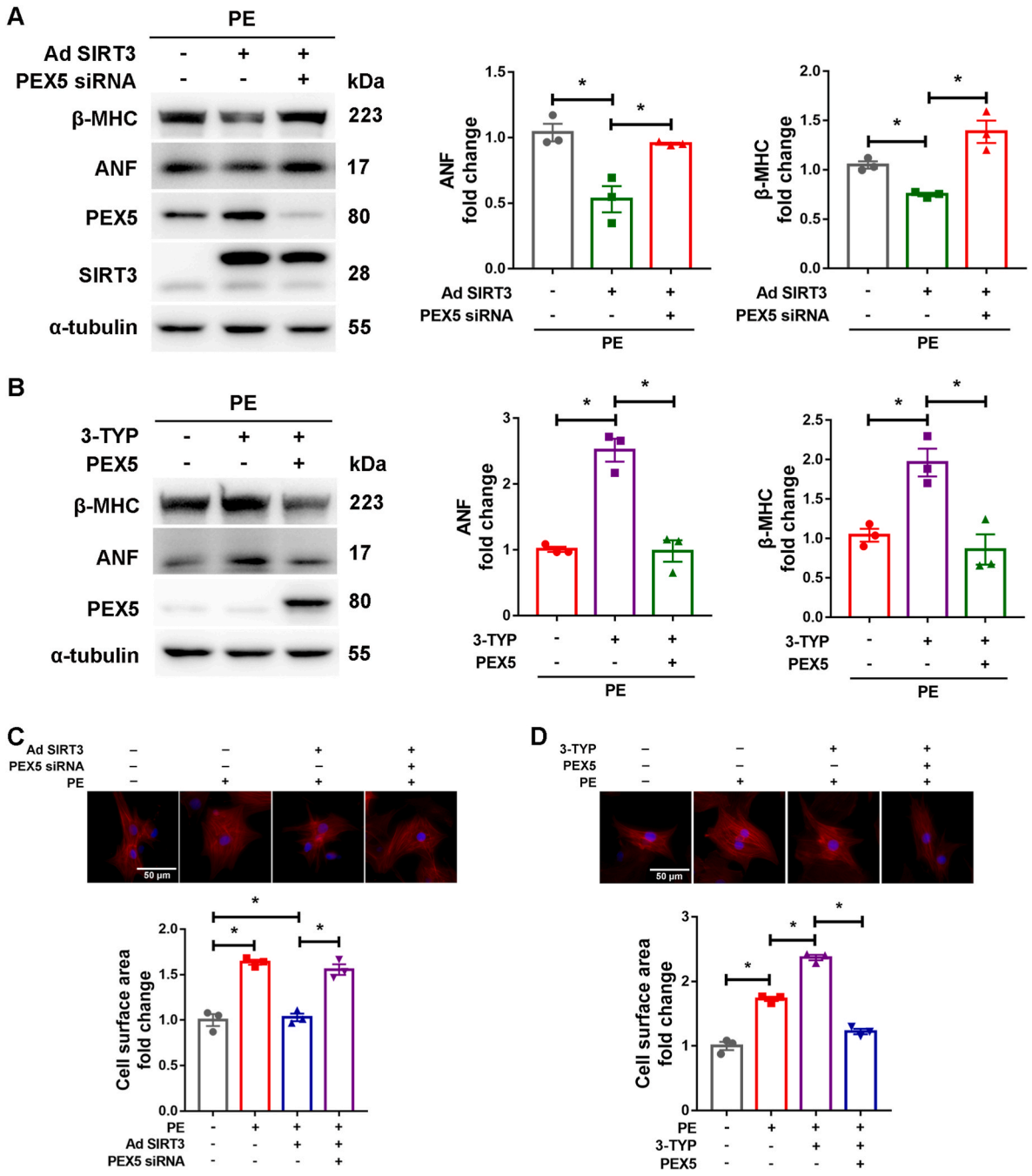

Fig. 2. PEX5 was involved in inhibitory effect of SIRT3 on cardiomyocyte hypertrophy. NRCMs were simultaneously infected with Ad SIRT3 and transfected with PEX5 siRNA in settings of PE (100 μM , 24h) treatment. Ad GFP was used as negative control to Ad SIRT3 and Ctrl siRNA was used as negative control to PEX5 siRNA **(A, C)**. Or NRCMs were simultaneously treated with SIRT3 inhibitor 3-TYP (50 μM, 12h) and transfected with Flag-PEX5 plasmid in settings of PE (100 μM , 24h) treatment. DMSO was used as negative control to 3-TYP and vector was used as negative control to Flag-PEX5 plasmid **(B, D)**. The protein level of hypertrophic marker ANF and β-MHC was detected by Western blot **(A, B)**. Cardiomyocyte surface area was examined by Rhodamine-Phalloidin staining and calculated by High-Content Screening System **(C, D)**. The data were presented as the means ± SEM. $^*P < 0.05$. $n = 3$.

These results indicated that PEX5 was required for the protective effects of SIRT3 on mitochondrial dynamics, structure and function against cardiomyocyte hypertrophy.

3.4. SIRT3 improved peroxisomal biogenesis and function via PEX5

PEX5 plays an essential role in peroxisomal biogenesis and maintaining peroxisomal structure and function [24,38]. Considering that SIRT3 regulates the expression of PEX5, it is hypothesized that SIRT3 could regulate peroxisomes via PEX5 in cardiomyocytes. Thus, peroxisomal biogenesis, ultrastructure, superoxide level and catalase content were detected to assess the regulatory role of SIRT3/PEX5. During cardiomyocyte hypertrophy, the peroxisomal membrane proteins PEX14 and PMP70 were downregulated, implying that peroxisomal biogenesis was repressed (Fig. 4A). SIRT3 overexpression abolished the PE-induced suppression of PEX14 and PMP70, while SIRT3 knockdown aggravated the impairment of peroxisomal biogenesis (Fig. 4B and C). Interestingly, SIRT3 regulated peroxisomal biogenesis via PEX5, as indicated by observations that si-PEX5 repressed the protective effect of SIRT3 on upregulating peroxisomal proteins and that

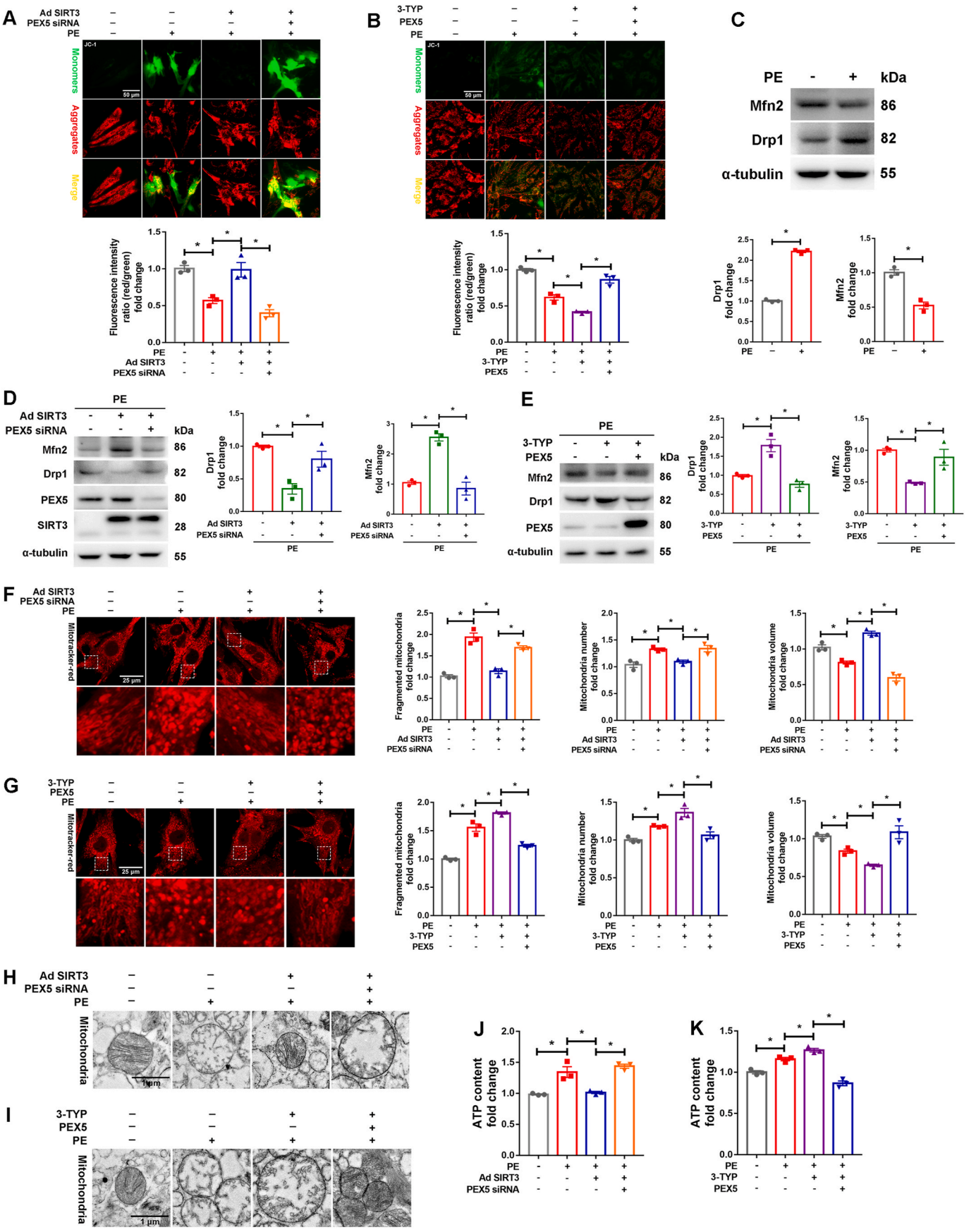

(caption on next page)

Fig. 3. PEX5 participated in SIRT3's protective effect of mitochondria fitness. (A) NRCMs were simultaneously infected with Ad SIRT3 and transfected with PEX5 siRNA followed by PE (100 μM , 24h) treatment. Ad GFP was used as negative control to Ad SIRT3 and Ctrl siRNA was used as negative control to PEX5 siRNA. Mitochondrial membrane potential was detected by JC-1 staining and calculated by High-Content Screening System. **(B)** NRCMs were treated with SIRT3 inhibitor 3-TYP (50 μM , 12h) and transfected with Flag-PEX5 plasmid followed by PE (100 μM , 24h) treatment. Mitochondrial membrane potential was detected by JC-1 staining and calculated by High-Content Screening System. **(C)** NRCMs were treated with PE (100 μM , 24h). Drp1 and Mfn2 was detected by Western blot. **(D)** NRCMs were simultaneously infected with Ad SIRT3 and transfected with PEX5 siRNA in the context of PE (100 μM , 24h) treatment. Ad GFP was used as negative control to Ad SIRT3 and Ctrl siRNA was used as negative control to PEX5 siRNA. Drp1 and Mfn2 was detected by Western blot. **(E)** NRCMs were treated with SIRT3 inhibitor 3-TYP (50 μM , 12h) and transfected with Flag-PEX5 plasmid in the context of PE (100 μM , 24h) treatment. Drp1 and Mfn2 was detected by Western blot. NRCMs were simultaneously infected with Ad SIRT3 and transfected with PEX5 siRNA followed by PE (100 μM , 24h) treatment. Ad GFP was used as negative control to Ad SIRT3 and Ctrl siRNA was used as negative control to PEX5 siRNA **(F, H, J)**. NRCMs were treated with SIRT3 inhibitor 3-TYP (50 μM , 12h) and transfected with Flag-PEX5 plasmid followed by PE (100 μM , 24h) treatment **(G, I, K)**. Mitochondrial network was detected by Mitotracker-red staining. Fluorescence images were acquired by Laser Scanning Confocal Microscope. Mitochondrial dynamic parameters were analyzed by ImageJ **(F, G)**. Mitochondrial ultrastructure was examined by TEM **(H, I)**. ATP content was measured by ATP assay kit **(J, K)**. The data were presented as the means ± SEM. $^*P < 0.05$. $n = 3$. (For interpretation of the references to colour in this figure legend, the reader is referred to the Web version of this article.)

PEX5 overexpression recovered the impairment of peroxisomal biogenesis induced by SIRT3 inhibition (Fig. 4D and E). In addition, TEM results showed that SIRT3 could preserve peroxisomal ultrastructure in cardiomyocytes via PEX5 (Fig. 4F and G). Under normal conditions, peroxisomes in cardiomyocytes were displayed as spherical or elliptical organelles with distinct crystal nuclei and complete single membranes; however, PE stimulation resulted in abnormalities in peroxisomal ultrastructure, including vague or absent crystal nuclei, incomplete organelle membranes and a more tenuous matrix (Fig. 4F and G). PEX5 silencing destroyed the protective effect of SIRT3 against PE-induced abnormalities in peroxisomal ultrastructure, whereas PEX5 overexpression improved peroxisomal structure in the presence of the SIRT3 inhibitor 3-TYP (Fig. 4F and G). Moreover, we also evaluated peroxisomal function by measuring superoxide levels through DHE staining and the expression level of catalase, which is a major peroxisome protein that removes superoxide. The superoxide level was prominently increased and catalase content was decreased following PE treatment (Fig. 4H and I), suggesting that peroxisomal function was disrupted and cellular oxidative stress was enhanced in cardiomyocyte hypertrophy. SIRT3 alleviated the increased superoxide level and reduced catalase expression, which was impaired when PEX5 was deficient (Fig. 4H and I). In contrast, PE-induced peroxisomal malfunction was aggravated by 3-TYP, but PEX5 overexpression attenuated this detrimental effect (Fig. 4G–I). These data provided solid evidence that SIRT3 protected peroxisomes via PEX5.

3.5. PEX5 was a key regulator of peroxisomes-mitochondria interplay

Based on the above results, PEX5 was involved in the regulatory effects of SIRT3 on both mitochondria and peroxisomes. However, it is still unclear how SIRT3/PEX5 drives the cross-interaction between these two organelles. SIRT3 is mainly located in the mitochondria, while PEX5 is a peroxisomal protein. Our observations that PEX5 was not localized in mitochondria (Fig. S3) might exclude the possibility that SIRT3 directly interacts with PEX5 in mitochondria. Recently, substantial evidence has been provided that peroxisomes and mitochondria exhibit functional interplay [30]. These findings prompted the hypothesis that PEX5 is a bridge linking mitochondria and peroxisomes. Deficiency of PEX5 might impair the biogenesis and function of peroxisomes, destroy the interplay between peroxisomes and mitochondria, and ultimately affect mitochondrial function. To test this hypothesis, PEX5 was knocked down or overexpressed in cardiomyocytes to investigate the changes in peroxisomal function and mitochondrial homeostasis.

In cardiomyocyte hypertrophy, PEX5 deficiency disrupted peroxisomal biogenesis (Fig. 5A), perturbed peroxisomal ultrastructure (Fig. 5C), augmented superoxide levels and decreased catalase content (Fig. 5E), confirming that peroxisomal defects could be induced by PEX5 insufficiency. Additionally, the transportation ability of PEX5 was suppressed during cardiomyocyte hypertrophy, as assessed by the reduced co-localization of PEX14 (a peroxisomal marker protein) and catalase (a major cargo protein of PEX5) (Fig. S4). In contrast, disorders in peroxisomal biogenesis, ultrastructure and function induced by PE could be rescued by PEX5 overexpression (Fig. 5B, D, F). These findings emphasized the important role of PEX5 in maintaining peroxisomal homeostasis.

To further investigate whether or not alteration of peroxisomes by PEX5 influences the peroxisomes-mitochondria interplay, mitochondrial functions were assessed. According to the results, PEX5 deficiency aggravated the decrease in MMP (Fig. 6A), mitochondrial fission (Fig. 6C), network fragmentation (Fig. 6E), ultrastructural destruction (Fig. 6G) and elevation of ATP levels (Fig. 6I) in hypertrophic cardiomyocytes. In contrast, mitochondrial damage induced by hypertrophic stimuli was alleviated by PEX5 overexpression (Fig. 6B, D, F. H, J). Therefore, these results provide evidence that PEX5 is a key regulator of the peroxisomes-mitochondria interplay.

Taken together, SIRT3 might improve peroxisomal biogenesis and function by preserving PEX5 expression; the improvement in peroxisomal homeostasis ultimately enhances mitochondrial function via organelle interplay.

4. Discussion

The present study identified a novel mechanism underlying the protective effect of SIRT3 against pathological cardiac hypertrophy, beyond its role as a deacetylase in mitochondria [2]. SIRT3 maintained peroxisome homeostasis by preserving the expression of the peroxisomal protein PEX5 and finally improved mitochondrial function via the peroxisomes-mitochondria interplay.

The regulation of PEX5 by SIRT3 was firstly observed by mRNA microarray analysis in SIRT3 knockout mice. PEX5 mRNA levels were significantly decreased in the hearts of *Sirt3*$^{-/-}$ mice, as well as in those of Ang II-induced cardiac hypertrophic mice, which displayed down-regulation of SIRT3. In line with the microarray data, the expression of PEX5 was attenuated in cardiomyocytes with SIRT3 silencing, whereas PEX5 expression was rebounded when SIRT3 was overexpressed (Fig. 1). The exact mechanism by which SIRT3 regulates PEX5 expression is still unclear. Considering the crucial role of SIRT3 in orchestrating mitochondria-nuclear retrograde signaling, it is most likely that the transcription of the PEX5 gene is altered by SIRT3-induced retrograde signals. In response to oxidative stress and proteotoxic stress during mitochondrial dysfunction, SIRT3 can trigger the UPR^{mt} retrograde response that alters the expression of nuclear genes involved in the antioxidant machinery and mitophagy as a complementary mechanism to the mitochondrial quality control system [12–14]. It is possible that SIRT3 could alter PEX5 expression by activating a variety of transcription factors involved in UPR^{mt}, including NRF2, ATF2, CREB, C/EBP, CHOP [10,11,39,40]. A second possibility is that SIRT3 could deacetylate and activate transcription factors or their co-regulators, such as PGC1α and FOXO3a [1,41], which are potentially responsible for transcription of the PEX family [42]. Alternatively, the other possibility is that SIRT3 is shuttled to the nucleus and modulates gene expression by deacetylating histones or non-histone proteins in nuclei [3,19]. Further

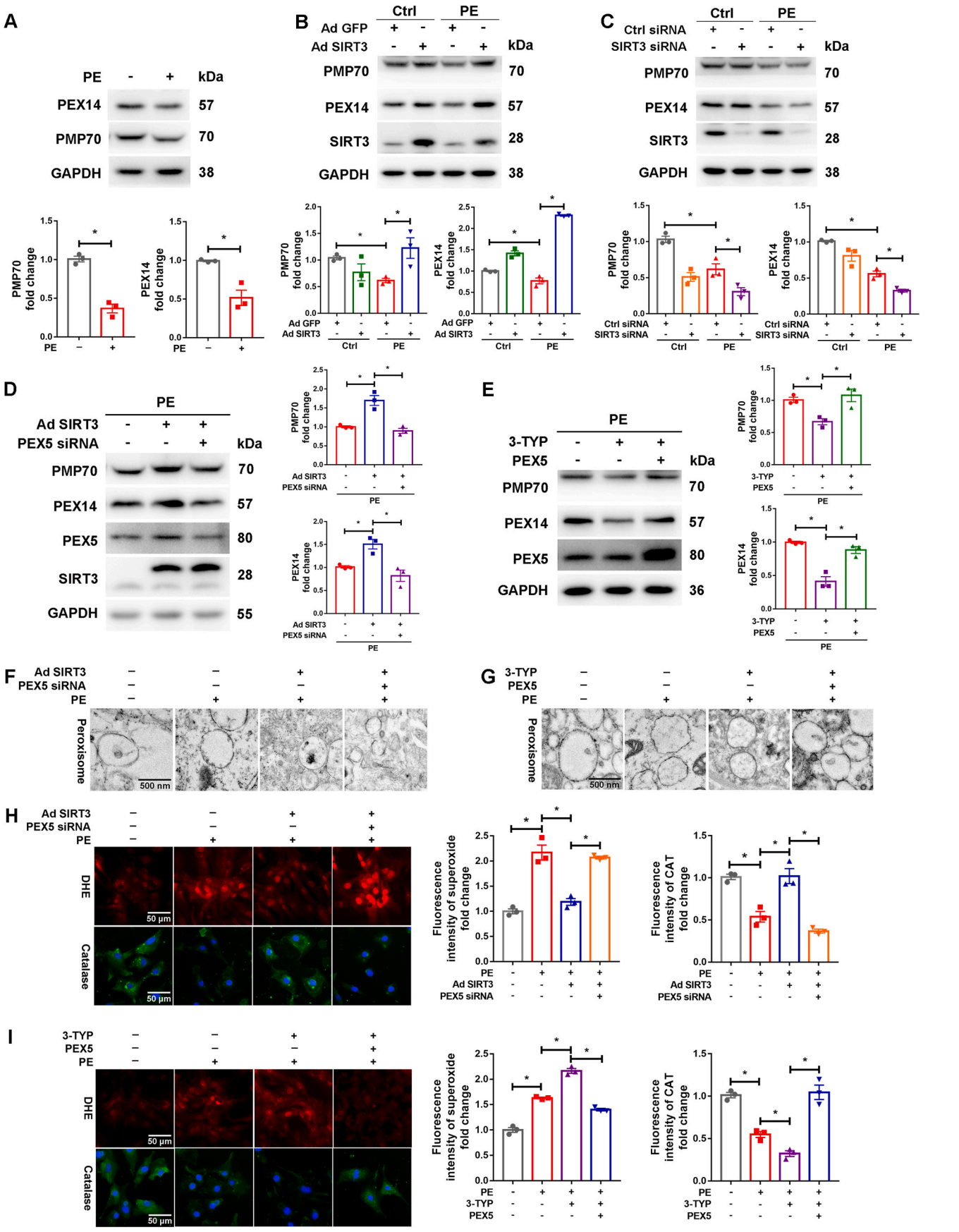

(caption on next page)

Fig. 4. SIRT3 improved peroxisomal biogenesis and function via promoting PEX5 expression. (A) NRCMs were treated with PE (100 μM , 24h). PEX14 and PMP70 was detected by Western blot. **(B)** NRCMs were infected by Ad SIRT3 with or without PE treatment. Protein level of peroxisomal biogenesis marker PEX14 and PMP70 were examined by Western blot. Ad GFP was used as negative control. **(C)** NRCMs were transfected with SIRT3 siRNA with or without PE treatment. Protein level of peroxisomal biogenesis marker PEX14 and PMP70 were examined by Western blot. Ctrl siRNA was used as negative control. **(D)** NRCMs were simultaneously infected with Ad SIRT3 and transfected with PEX5 siRNA in the context of PE (100 μM , 24h) treatment. Ad GFP was used as negative control to Ad SIRT3 and Ctrl siRNA was used as negative control to PEX5 siRNA. Protein level of peroxisomal biogenesis marker PEX14 and PMP70 were examined by Western blot. **(E)** NRCMs were treated with SIRT3 inhibitor 3-TYP (50 μM , 12h) and transfected with Flag-PEX5 plasmid in the context of PE (100 μM , 24h) treatment. Protein level of peroxisomal biogenesis marker PEX14 and PMP70 were examined by Western blot. **(F)** NRCMs were simultaneously infected with Ad SIRT3 and transfected with PEX5 siRNA followed by PE (100 μM , 24h) treatment. Ad GFP was used as negative control to Ad SIRT3 and Ctrl siRNA was used as negative control to PEX5 siRNA. Peroxisomal ultrastructure was examined by TEM. **(G)** NRCMs were treated with SIRT3 inhibitor 3-TYP (50 μM , 12h) and transfected with Flag-PEX5 plasmid followed by PE (100 μM , 24h) treatment. Peroxisomal ultrastructure was examined by TEM. **(H)** NRCMs were simultaneously infected with Ad SIRT3 and transfected with PEX5 siRNA followed by PE (100 μM , 24h) treatment. Ad GFP was used as negative control to Ad SIRT3 and Ctrl siRNA was used as negative control to PEX5 siRNA. Superoxide level was detected by DHE staining and catalase content was measured by immuno-fluorescence. **(I)** NRCMs were treated with SIRT3 inhibitor 3-TYP (50 μM , 12h) and transfected with Flag-PEX5 plasmid followed by PE (100 μM , 24h) treatment. Superoxide level was detected by DHE staining and catalase content was measured by immuno-fluorescence. CAT: catalase. The data were presented as the means ± SEM. $^*P < 0.05$. $n = 3$.

investigations are required to explore how SIRT3 regulates PEX5 expression in the future. It is also noted that SIRT3 deficiency might result in impairments in mitochondrial retrograde signaling, ultimately repressing the expression of PEX5 under pathological conditions.

Most importantly, our data support the conclusion that PEX5 is involved in the protective effect of SIRT3 against cardiomyocyte hypertrophy. Knockdown of PEX5 reversed the inhibitory effect of SIRT3 on hypertrophic markers and cardiomyocyte size; on the contrary, overexpression of PEX5 alleviated the hypertrophic response induced by SIRT3 inhibition (Fig. 2). The cardioprotective effects of SIRT3 are closely associated with the preservation of mitochondrial homeostasis during cardiac hypertrophy [37]. Surprisingly, PEX5 also participates in mitochondrial regulation by SIRT3. This is supported by the observations that PEX5 silencing destroyed the beneficial effect of SIRT3 on the mitochondrial membrane potential, mitochondrial dynamic balance, mitochondrial morphology and ultrastructure, and ATP production, and that PEX5 overexpression rescued the morphological and functional impairment of mitochondria caused by SIRT3 inhibition (Fig. 3).

Since PEX5 is a shuttling import receptor for peroxisomal matrix proteins and is mainly located at the peroxisomal membrane [24], it is critical to determine the mechanisms by which PEX5 modulates mitochondrial function. It seems unlikely that PEX5 could directly interact with SIRT3 to influence mitochondrial structure and function, in view of the fact that PEX5 was not located in mitochondria (Fig. S3). PEX5 is essential for peroxisomal biogenesis and maintenance, considering that PEX5 deficiency suppressed peroxisomal biogenesis, damaged peroxisomal ultrastructure, increased cellular oxidative stress, and reduced catalase content (Fig. 5). These results are consistent with previous observations that PEX5 deletion triggered peroxisomal dysfunction in mice [26] or in patients [27]. Interestingly, peroxisomes are implicated in functional cooperation with mitochondria in the regulation of fatty acid metabolism and the maintenance of cellular superoxide homeostasis and organelle membrane dynamics [30,43,44]. This finding thus prompted the hypothesis that PEX5 might act as a regulator of the peroxisomes-mitochondria interplay. Indeed, PEX5 deficiency not only leads to peroxisomal defects but also damages mitochondrial homeostasis, as implied by the results that PEX5 knockdown aggravated the decrease in mitochondrial membrane potential, imbalance of mitochondrial fission and fusion, network fragmentation and ultrastructural destruction, and abnormal production of ATP in hypertrophic cardiomyocytes (Fig. 6). In line with our observations, ample evidence from *in vivo* and *in vitro* studies supports that PEX5 deficiency could result in mitochondrial damage. In *Pex5*$^{-/-}$ mice and Zellweger syndrome patients, mitochondrial abnormalities, including ultrastructural defects, decreased MMP, suppression of the mitochondrial respiratory chain, and elevated production of superoxide, were observed in the liver, kidney, and neutrophils [27,45,46].

We further investigated whether SIRT3 regulates peroxisomes-mitochondria crosstalk via PEX5 during cardiac hypertrophy. In response to hypertrophic stimuli, peroxisomes in cardiomyocytes developed biogenesis disorder and functional impairment, as reflected by the downregulation of peroxisomal membrane proteins, abnormalities of peroxisomal ultrastructure, repression of peroxisomal catalase and excessive production of superoxide (Fig. 4 & Fig. S4). These peroxisomal abnormalities were alleviated by SIRT3 overexpression but were exacerbated following SIRT3 inhibition, supporting that SIRT3 contributes to preserving peroxisomal homeostasis in cardiomyocyte hypertrophy (Fig. 4). Notably, downregulation of PEX5 reversed the beneficial effect of SIRT3, while upregulation of PEX5 improved SIRT3 inhibitor-induced peroxisomal impairment (Fig. 4). Combining the evidence that PEX5 participates in the regulation of peroxisomes-mitochondria interactions, these findings shed new light on the SIRT3/PEX5 regulatory axis in modulating the peroxisomes-mitochondria interplay. During the pathogenesis of cardiomyocyte hypertrophy, SIRT3 deficiency might lead to downregulation of PEX5, which facilitates peroxisomal defects and finally results in mitochondrial dysfunction via the cross-interaction between these two organelles. Strategies targeting activation or upregulation of the SIRT3/PEX5 axis might suggest therapeutic potential in pathological cardiac hypertrophy by improving the peroxisomes-mitochondria interplay.

Currently, the molecular basis of mitochondria-peroxisomes interconnectivity remains to be addressed. Coexisting in the cytoplasm, peroxisomes and mitochondria communicate with each other probably through direct interorganelle contact, diffusion of molecular messengers (including H_2O_2, lipids, metabolites and proteins), or vesicular trafficking [30,47]. The first possibility is that key fission components are shared by both organelles during organelle division; secondly, since H_2O_2, the main oxidative byproduct in peroxisomes, can trigger redox-dependent mitochondrial and cellular superoxide production [48], peroxisome-derived catalase possibly participates in H_2O_2 metabolism and helps to modulate mitochondrial redox homeostasis; thirdly, long-chain fatty acid metabolism by peroxisomal β-oxidation is involved in lipotoxicity, which is a leading cause of mitochondrial impairment; and last but not least, possibility also exists in information communication, mainly via vesicle transport, between these two organelles [30,47]. Further investigation should be conducted to determine the exact mechanism underlying the SIRT3/PEX5-regulated peroxisomes-mitochondria interplay.

5. Conclusion

The present study unveils a previously unrecognized role of SIRT3 in modulating the peroxisomes-mitochondra interplay in cardiac hypertrophy by preserving PEX5 expression. These findings identify a novel mechanism underlying the protective role of SIRT3 against pathological cardiac hypertrophy, and provide a more comprehensive understanding of SIRT3 in mitochondrial regulation via interorganelle communication.

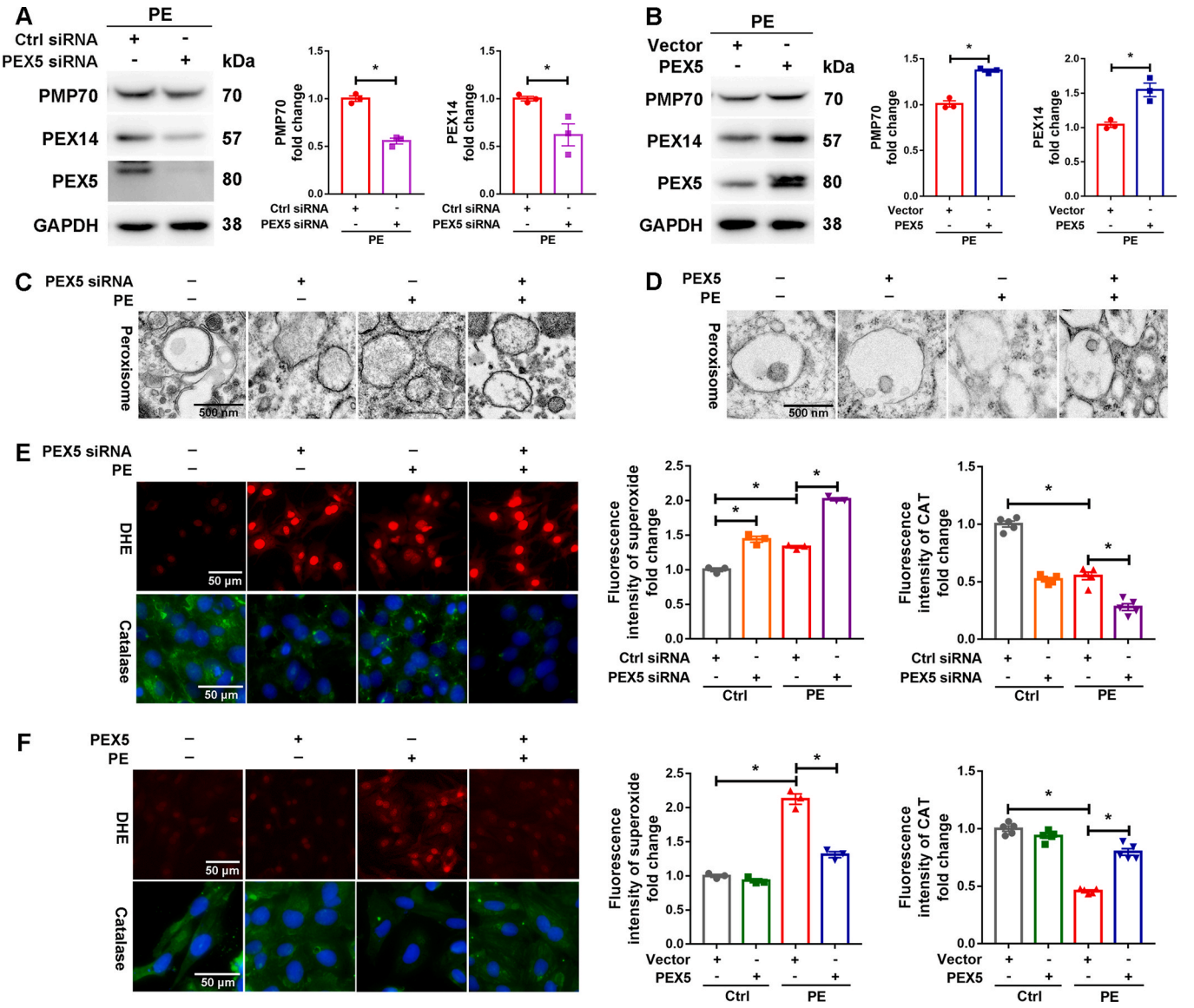

Fig. 5. Downregulation of PEX5 led to peroxisomal deficiency in cardiomyocytes. (A) NRCMs were transfected with PEX5 siRNA in the context of PE (100 μM，24h) treatment. Ctrl siRNA was used as negative control. Protein level of peroxisomal biogenesis marker PEX14 and PMP70 were examined by Western blot. **(B)** NRCMs were transfected with PEX5-Flag plasmid in the context of PE (100 μM，24h) treatment. Vector was used as negative control. Protein level of peroxisomal biogenesis marker PEX14 and PMP70 were examined by Western blot. **(C)** NRCMs were transfected with PEX5 siRNA followed by PE (100 μM，24h) treatment. Ctrl siRNA was used as negative control. Peroxisomal ultrastructure was examined by TEM. **(D)** NRCMs were transfected with PEX5-Flag plasmid followed by PE (100 μM，24h) treatment. Vector was used as negative control. Peroxisomal ultrastructure was examined by TEM. $^*P < 0.05$. $n = 3$ **(E)** NRCMs were transfected with PEX5 siRNA followed by PE (100 μM，24h) treatment. Ctrl siRNA was used as negative control. Superoxide level was detected by DHE staining ($^*P < 0.05$. $n = 3$) and catalase content was measured by immuno-fluorescence ($^*P < 0.05$. $n = 5$). CAT: catalase. **(F)** NRCMs were transfected with PEX5-Flag plasmid followed by PE (100 μM，24h) treatment. Vector was used as negative control. Superoxide level was detected by DHE staining ($^*P < 0.05$. $n = 3$) and catalase content was measured by immuno-fluorescence ($^*P < 0.05$. $n = 5$). CAT: catalase. The data were presented as the means ± SEM.

Author contributions

Minghui Wang and Yanqing Ding performed the research and wrote the manuscript. Zeyu Li, Yuehuai Hu and Wenwei Luo performed the research and analyzed the data. Zhuoming Li and Peiqing Liu designed the study, reviewed and approved the research protocol and wrote the manuscript. Zhuoming Li and Peiqing Liu are the guarantors of this work and, as such, had full access to all the data in the study and took responsibility for the integrity of the data and the accuracy of the data analysis.

Submission declaration and verification

All authors declare that this manuscript is original, that the work described has not been published previously, that it is not under consideration for publication elsewhere, that its publication is approved by all authors and tacitly or explicitly by the responsible authorities where the work was carried out, and that, if accepted, it will not be published elsewhere in the same form, in English or in any other language, including electronically without the written consent of the copyright-holder.

We confirm that the manuscript has been read and approved by all named authors and that there are no other persons who satisfied the criteria for authorship but are not listed. We further confirm that the

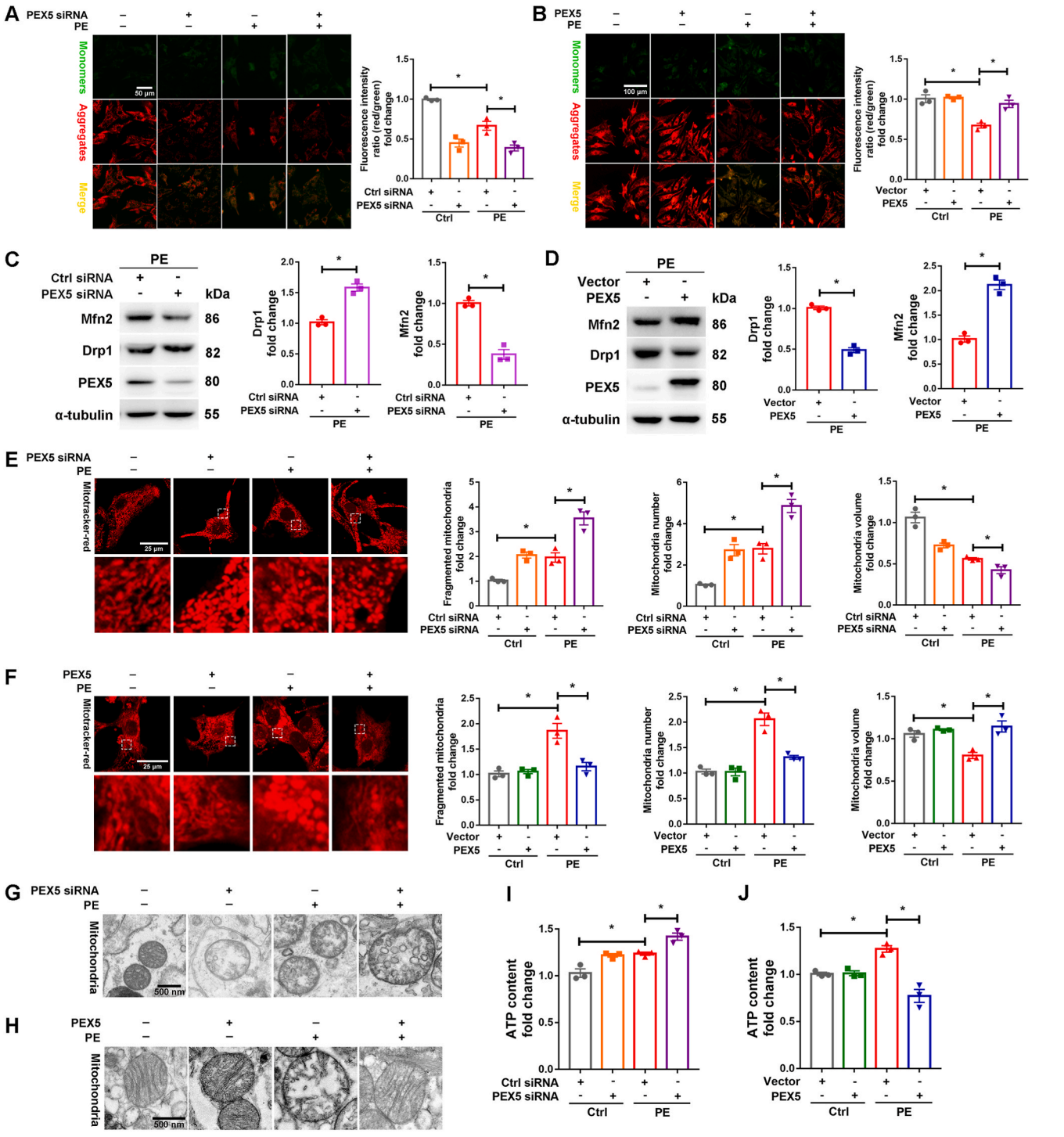

Fig. 6. Peroxisomal deficiency disrupted mitochondria homeostasis in cardiomyocyte. (A) NRCMs were infected transfected with PEX5 siRNA with or without PE (100 μM, 24h) treatment. Mitochondria membrane potential was detected by JC-1 staining. **(B)** NRCMs were transfected with Flag-PEX5 Plasmid with or without PE (100 μM, 24h) treatment. Mitochondria membrane potential was detected by JC-1 staining. **(C)** NRCMs were transfected with PEX5 siRNA in the context of PE (100 μM, 24h) treatment. Ctrl siRNA was used as negative control. Protein level of Drp1 and Mfn2 was detected by Western blot. **(D)** NRCMs were transfected with Flag-PEX 5plasmind with or without PE (100 μM , 24h) treatment. Vector was used as negative control. Protein level of Drp1 and Mfn2 was detected by Western blot. **(E)** NRCMs were transfected with PEX5 siRNA with or without PE (100 μM , 24h) treatment. Ctrl siRNA was used as negative control. Mitochondria network was detected by Mitotracker-red staining. **(F)** NRCMs were transfected with Flag-PEX5 plasmid with or without PE (100 μM , 24h) treatment. Mitochondria network was detected by Mitotracker-red staining. **(G)** NRCMs were transfected with PEX5 siRNA with or without PE (100 μM , 24h) treatment. Ctrl siRNA was used as negative control. Mitochondria ultrastructure was examined by TEM. **(H)** NRCMs were transfected with Flag-PEX5 plasmid with or without PE (100 μM , 24h) treatment. Mitochondria ultrastructure was examined by TEM. **(I)** NRCMs were transfected with PEX5 siRNA with or without PE (100 μM , 24h) treatment. Ctrl siRNA was used as negative control. ATP content was measured by ATP assay kit. **(J)** NRCMs were transfected with Flag-PEX5 plasmid with or without PE (100 μM , 24h) treatment. ATP content was measured by ATP assay kit. The data were presented as the means ± SEM. $^*P < 0.05$. $n = 3$. (For interpretation of the references to colour in this figure legend, the reader is referred to the Web version of this article.)

order of authors listed in the manuscript has been approved by all of us.

We understand that the Corresponding Author is the sole contact for the Editorial process. He/she is responsible for communicating with the other authors about progress, submissions of revisions and final approval of proofs.

We declare no conflict of interests.

Conflict of interest statement

The authors confirm that there are no conflicts of interest regarding the publication of this article.

Data availability

Data will be made available on request.

Acknowledgements

The study is supported by grants from Guangdong Basic and Applied Basic Research Foundation [2022A1515011374], Guangxi Natural Science Foundation [2022GXNSFDA080001], National Natural Science Foundation of China [82273925, U21A20419, 81973318], Local Innovative and Research Teams Project of Guangdong Pearl River Talents Program [2017BT01Y093], National Engineering and Technology Research Center for New drug Druggability Evaluation (Seed Program of Guangdong Province) [2017B090903004], and Guangdong Provincial Key Laboratory of Construction Foundation [2017B030314030], National Natural Science Foundation of China [82003746], Guangdong Basic and Applied Basic Research Foundation [2023A1515011133].

Appendix A. Supplementary data

Supplementary data to this article can be found online at https://doi.org/10.1016/j.redox.2023.102652.

References

[1] W. Sun, C. Liu, Q. Chen, N. Liu, Y. Yan, B. Liu, SIRT3: A New Regulator of Cardiovascular Diseases [J], 2018, Oxid Med Cell Longev, 2018, 7293861.
[2] V.B. Pillai, N.R. Sundaresan, V. Jeevanandam, M.P. Gupta, Mitochondrial SIRT3 and heart disease [J], Cardiovasc. Res. 88 (2) (2010) 250–256.
[3] N.R. Sundaresan, M. Gupta, G. Kim, S.B. Rajamohan, A. Isbatan, M.P. Gupta, Sirt3 blocks the cardiac hypertrophic response by augmenting Foxo3a-dependent antioxidant defense mechanisms in mice [J], J. Clin. Invest. 119 (9) (2009) 2758–2771.
[4] M.N. Sack, Emerging characterization of the role of SIRT3-mediated mitochondrial protein deacetylation in the heart [J], Am. J. Physiol. Heart Circ. Physiol. 301 (6) (2011) H2191–H2197.
[5] S. Someya, W. Yu, W.C. Hallows, J. Xu, J.M. Vann, C. Leeuwenburgh, M. Tanokura, J.M. Denu, T.A. Prolla, Sirt3 mediates reduction of oxidative damage and prevention of age-related hearing loss under caloric restriction [J], Cell 143 (5) (2010) 802–812.
[6] A.E. Dikalova, H.A. Itani, R.R. Nazarewicz, W.G. McMaster, C.R. Flynn, R. Uzhachenko, J.P. Fessel, J.L. Gamboa, D.G. Harrison, S.I. Dikalov, Sirt3 impairment and SOD2 Hyperacetylation in Vascular oxidative stress and hypertension [J], Circ. Res. 121 (5) (2017) 564–574.
[7] B.H. Ahn, H.S. Kim, S. Song, I.H. Lee, J. Liu, A. Vassilopoulos, C.X. Deng, T. Finkel, A role for the mitochondrial deacetylase Sirt3 in regulating energy homeostasis [J], Proc. Natl. Acad. Sci. U. S. A. 105 (38) (2008) 14447–14452.
[8] M.D. Hirschey, T. Shimazu, E. Goetzman, E. Jing, B. Schwer, D.B. Lombard, C. A. Grueter, C. Harris, S. Biddinger, O.R. Ilkayeva, R.D. Stevens, Y. Li, A.K. Saha, N. B. Ruderman, J.R. Bain, C.B. Newgard, R.V. Farese Jr., F.W. Alt, C.R. Kahn, E. Verdin, SIRT3 regulates mitochondrial fatty-acid oxidation by reversible enzyme deacetylation [J], Nature 464 (7285) (2010) 121–125.
[9] S.A. Samant, H.J. Zhang, Z. Hong, V.B. Pillai, N.R. Sundaresan, D. Wolfgeher, S. L. Archer, D.C. Chan, M.P. Gupta, SIRT3 deacetylates and activates OPA1 to regulate mitochondrial dynamics during stress [J], Molecular and cellular biology 34 (5) (2014) 807–819.
[10] R.A. Butow, N.G. Avadhani, Mitochondrial signaling: the retrograde response [J], Mol Cell 14 (1) (2004) 1–15.
[11] P.M. Quiros, A. Mottis, J. Auwerx, Mitonuclear communication in homeostasis and stress [J], Nat. Rev. Mol. Cell Biol. 17 (4) (2016) 213–226.
[12] L. Papa, D. Germain, SirT3 regulates the mitochondrial unfolded protein response [J], Molecular and cellular biology 34 (4) (2014) 699–710.
[13] H. Chen, D.M. Zhang, Z.P. Zhang, M.Z. Li, H.F. Wu, SIRT3-mediated mitochondrial unfolded protein response weakens breast cancer sensitivity to cisplatin [J], Genes Genomics 43 (12) (2021) 1433–1444.
[14] M. Xu, R.Q. Xue, Y. Lu, S.Y. Yong, Q. Wu, Y.L. Cui, X.T. Zuo, X.J. Yu, M. Zhao, W. J. Zang, Choline ameliorates cardiac hypertrophy by regulating metabolic remodelling and UPRmt through SIRT3-AMPK pathway [J], Cardiovasc. Res. 115 (3) (2019) 530–545.
[15] W. Yu, B. Gao, N. Li, J. Wang, C. Qiu, G. Zhang, M. Liu, R. Zhang, C. Li, G. Ji, Y. Zhang, Sirt3 deficiency exacerbates diabetic cardiac dysfunction: role of Foxo3A-Parkin-mediated mitophagy [J], Biochim. Biophys. Acta, Mol. Basis Dis. 1863 (8) (2017) 1973–1983.
[16] J. Li, T. Chen, M. Xiao, N. Li, S. Wang, H. Su, X. Guo, H. Liu, F. Yan, Y. Yang, Y. Zhang, P. Bu, Mouse Sirt3 promotes autophagy in AngII-induced myocardial hypertrophy through the deacetylation of FoxO1 [J], Oncotarget 7 (52) (2016) 86648–86659.
[17] N.R. Sundaresan, S. Bindu, V.B. Pillai, S. Samant, Y. Pan, J.Y. Huang, M. Gupta, R. S. Nagalingam, D. Wolfgeher, E. Verdin, M.P. Gupta, SIRT3 blocks Aging-associated tissue fibrosis in mice by deacetylating and activating Glycogen Synthase Kinase 3beta [J], Molecular and cellular biology 36 (5) (2015) 678–692.
[18] J. Bao, Z. Lu, J.J. Joseph, D. Carabenciov, C.C. Dimond, L. Pang, L. Samsel, J. P. McCoy Jr., J. Leclerc, P. Nguyen, D. Gius, M.N. Sack, Characterization of the murine SIRT3 mitochondrial localization sequence and comparison of mitochondrial enrichment and deacetylase activity of long and short SIRT3 isoforms [J], J. Cell. Biochem. 110 (1) (2010) 238–247.
[19] M.B. Scher, A. Vaquero, D. Reinberg, SirT3 is a nuclear NAD+-dependent histone deacetylase that translocates to the mitochondria upon cellular stress [J], Genes Dev. 21 (8) (2007) 920–928.
[20] T. Iwahara, R. Bonasio, V. Narendra, D. Reinberg, SIRT3 functions in the nucleus in the control of stress-related gene expression [J], Molecular and cellular biology 32 (24) (2012) 5022–5034.
[21] X. Feng, Y. Wang, W. Chen, S. Xu, L. Li, Y. Geng, A. Shen, H. Gao, L. Zhang, S. Liu, SIRT3 inhibits cardiac hypertrophy by regulating PARP-1 activity [J], Aging (Albany NY) 12 (5) (2020) 4178–4192.
[22] X. Palomer, M.S. Roman-Azcona, J. Pizarro-Delgado, A. Planavila, F. Villarroya, B. Valenzuela-Alcaraz, F. Crispi, A. Sepulveda-Martinez, I. Miguel-Escalada, J. Ferrer, J.F. Nistal, R. Garcia, M.M. Davidson, E. Barroso, M. Vazquez-Carrera, SIRT3-mediated inhibition of FOS through histone H3 deacetylation prevents cardiac fibrosis and inflammation [J], Signal Transduct Tar 5 (1) (2020).
[23] N.R. Sundaresan, S.A. Samant, V.B. Pillai, S.B. Rajamohan, M.P. Gupta, SIRT3 is a stress-responsive deacetylase in cardiomyocytes that protects cells from stress-mediated cell death by deacetylation of Ku70 [J], Molecular and cellular biology 28 (20) (2008) 6384–6401.
[24] T. Francisco, T.A. Rodrigues, M.O. Freitas, C.P. Grou, A.F. Carvalho, C. Sa-Miranda, M.P. Pinto, J.E. Azevedo, A cargo-centered perspective on the PEX5 receptor-mediated peroxisomal protein import pathway [J], J. Biol. Chem. 288 (40) (2013) 29151–29159.
[25] X. Liu, C. Ma, S. Subramani, Recent advances in peroxisomal matrix protein import [J], Curr. Opin. Cell Biol. 24 (4) (2012) 484–489.
[26] M. Baes, P. Gressens, E. Baumgart, P. Carmeliet, M. Casteels, M. Fransen, P. Evrard, D. Fahimi, P.E. Declercq, D. Collen, P.P. van Veldhoven, G.P. Mannaerts, A mouse model for Zellweger syndrome [J], Nat. Genet. 17 (1) (1997) 49–57.
[27] E. Baumgart, I. Vanhorebeek, M. Grabenbauer, M. Borgers, P.E. Declercq, H. D. Fahimi, M. Baes, Mitochondrial alterations caused by defective peroxisomal biogenesis in a mouse model for Zellweger syndrome (PEX5 knockout mouse) [J], Am. J. Pathol. 159 (4) (2001) 1477–1494.
[28] J.T. Koh, H.H. Choi, K.Y. Ahn, J.U. Kim, J.H. Kim, J.Y. Chun, Y.H. Baik, K.K. Kim, Cardiac characteristics of transgenic mice overexpressing Refsum disease gene-associated protein within the heart [J], Biochem Bioph Res Co 286 (5) (2001) 1107–1116.
[29] R.J. Wanders, J. C. Komen Peroxisomes, Refsum's disease and the alpha- and omega-oxidation of phytanic acid [J], Biochem. Soc. Trans. 35 (Pt 5) (2007) 865–869.
[30] M. Schrader, J. Costello, L.F. Godinho, M. Islinger, Peroxisome-mitochondria interplay and disease [J], J. Inherit. Metab. Dis. 38 (4) (2015) 681–702.
[31] N. Livnat-Levanon, M.H. Glickman, Ubiquitin-proteasome system and mitochondria - reciprocity [J], Biochim. Biophys. Acta 1809 (2) (2011) 80–87.
[32] A. Chaudhry, R. Shi, D.S. Luciani, A pipeline for multidimensional confocal analysis of mitochondrial morphology, function, and dynamics in pancreatic beta-cells [J], Am. J. Physiol. Endocrinol. Metab. 318 (2) (2020) E87–E101.
[33] Q. Zhou, L.L. Pan, R. Xue, G. Ni, Y. Duan, Y. Bai, C. Shi, Z. Ren, C. Wu, G. Li, B. Agerberth, J.P. Sluijter, J. Sun, J. Xiao, The anti-microbial peptide LL-37/CRAMP levels are associated with acute heart failure and can attenuate cardiac dysfunction in multiple preclinical models of heart failure [J], Theranostics 10 (14) (2020) 6167–6181.
[34] Z. Yue, Y. Ma, J. You, Z. Li, Y. Ding, P. He, X. Lu, J. Jiang, S. Chen, P. Liu, NMNAT3 is involved in the protective effect of SIRT3 in Ang II-induced cardiac hypertrophy [J], Exp. Cell Res. 347 (2) (2016) 261–273.
[35] Y.Q. Ding, Y.H. Zhang, J. Lu, B. Li, W.J. Yu, Z.B. Yue, Y.H. Hu, P.X. Wang, J.Y. Li, S. D. Cai, J.T. Ye, P.Q. Liu, MicroRNA-214 contributes to Ang II-induced cardiac hypertrophy by targeting SIRT3 to provoke mitochondrial malfunction [J], Acta Pharmacol. Sin. 42 (9) (2021) 1422–1436.
[36] M. Wang, J. Li, Y. Ding, S. Cai, Z. Li, P. Liu, PEX5 prevents cardiomyocyte hypertrophy via suppressing the redox-sensitive signaling pathways MAPKs and STAT3 [J], Eur. J. Pharmacol. 906 (2021), 174283.
[37] R.M. Parodi-Rullán, X.R. Chapa-Dubocq, S. Javadov, Acetylation of mitochondrial proteins in the heart: the role of SIRT3 [J], Front. Physiol. 9 (2018) 1094.

[38] M.L. Skowyra, T.A. Rapoport, PEX5 translocation into and out of peroxisomes drives matrix protein import [J], Mol Cell 82 (17) (2022) 3209–3225 e3207.
[39] F.M. da Cunha, N.Q. Torelli, A.J. Kowaltowski, Mitochondrial retrograde signaling: Triggers, pathways, and Outcomes [J], Oxid. Med. Cell. Longev. 2015 (2015), 482582.
[40] V. Jovaisaite, L. Mouchiroud, J. Auwerx, The mitochondrial unfolded protein response, a conserved stress response pathway with implications in health and disease [J], J. Exp. Biol. 217 (Pt 1) (2014) 137–143.
[41] H.C. Chang, L. Guarente, SIRT1 and other sirtuins in metabolism [J], Trends in endocrinology and metabolism: TEM (Trends Endocrinol. Metab.) 25 (3) (2014) 138–145.
[42] T.Y. Huang, D. Zheng, R.C. Hickner, J.J. Brault, R.N. Cortright, Peroxisomal gene and protein expression increase in response to a high-lipid challenge in human skeletal muscle [J], Metabolism 98 (2019) 53–61.
[43] J.C. Farré, S.S. Mahalingam, M. Proietto, S. Subramani, Peroxisome biogenesis, membrane contact sites, and quality control [J], EMBO Rep. 20 (1) (2019).
[44] M. Schrader, M. Kamoshita, M. Islinger, Organelle interplay-peroxisome interactions in health and disease [J], J. Inherit. Metab. Dis. 43 (1) (2020) 71–89.
[45] A. Peeters, A.B. Shinde, R. Dirkx, J. Smet, K. De Bock, M. Espeel, I. Vanhorebeek, A. Vanlander, R. Van Coster, P. Carmeliet, M. Fransen, P.P. Van Veldhoven, M. Baes, Mitochondria in peroxisome-deficient hepatocytes exhibit impaired respiration, depleted DNA, and PGC-1 alpha independent proliferation [J], Bba-Mol Cell Res 1853 (2) (2015) 285–298.
[46] H. Tanaka, T. Okazaki, S. Aoyama, M. Yokota, M. Koike, Y. Okada, Y. Fujiki, Y. Gotoh, Peroxisomes control mitochondrial dynamics and the mitochondrion-dependent apoptosis pathway [J], J. Cell Sci. 132 (11) (2019).
[47] M. Fransen, C. Lismont, P. Walton, The peroxisome-mitochondria Connection: how and Why? [J], Int. J. Mol. Sci. 18 (6) (2017).
[48] S.I. Dikalov, R.R. Nazarewicz, A. Bikineyeva, L. Hilenski, B. Lassegue, K. K. Griendling, D.G. Harrison, A.E. Dikalova, Nox2-induced production of mitochondrial superoxide in angiotensin II-mediated endothelial oxidative stress and hypertension [J], Antioxidants Redox Signal. 20 (2) (2014) 281–294.